

Comparison between C-band and S-band radar rainfall for hydrological simulations in Marikina River Basin, Philippines

Catherine Abon¹, Irene Crisologo², David Kneis¹, Axel Bronstert¹, and Maik Heistermann¹

¹University of Potsdam, Institute of Earth and Environmental Sciences, Karl-Liebknecht-Str. 24-25, 14476 Potsdam, Germany

²University of the Philippines Diliman, National Institute of Geological Sciences, Environment Monitoring Laboratory, Quezon City, 1101 Philippines

(Dated: 18 July 2014)



Catherine Abon

1 Introduction

With over 13 million inhabitants, Metro Manila is one of the most densely populated cities in the world. Being the country's main economic center, it is a critical hub for industrial and services infrastructure development. Unfortunately, it suffers from huge economic losses caused by frequent floods that damage these infrastructures. In August 2012, a heavy rainfall of almost 800 mm accumulated depth in roughly four days occurred in Metro Manila and nearby towns, inflicting a damage cost of around US\$ 70M, 109 confirmed deaths, and more than 776,000 displaced (NDRRMC, 2013). This event was brought by the southwest monsoon (locally known as *Habagat*) and enhanced by the passage of a typhoon north of the Philippines.

The Marikina River Basin (MRB) has an area of 535 km², making it the largest among seven river basins in Metro Manila (Fig.1) and poses the most serious flood hazard to the region (Liongson, 2008). The mean annual precipitation is 2400 mm and potential evapotranspiration is 1500 mm (PAGASA, 2004). In December 2011, the government launched the Nationwide Operational Assessment of Hazard (project-NOAH). This involved the deployment of new monitoring equipment (such as over 1000 new rain gauges and new weather radar stations), active research and development in forecasting (e.g. Heistermann et al. 2013a), and dissemination of real-time hydro-meteorological information in the Internet (<http://noah.dost.gov.ph>).

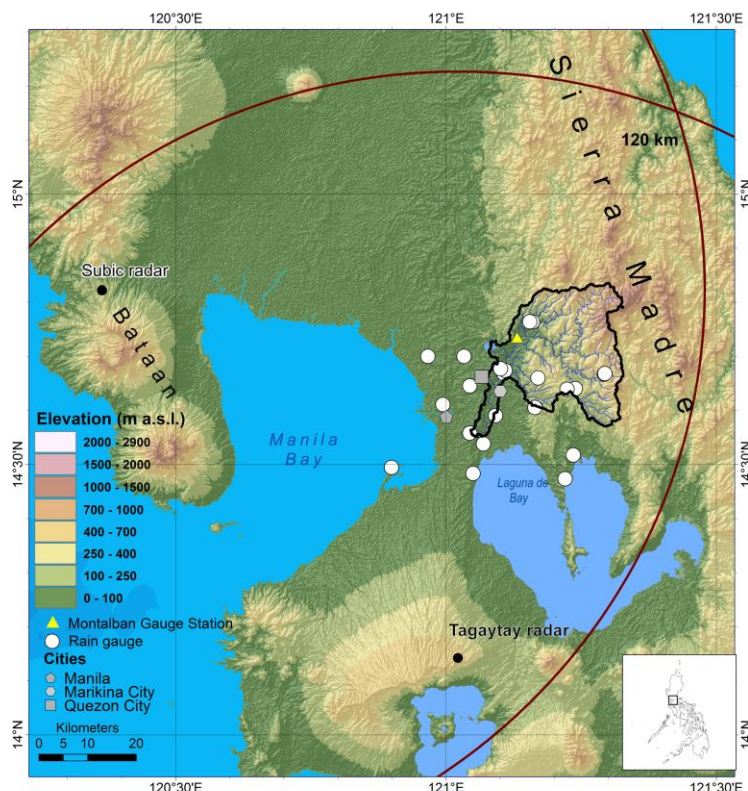


Figure 1: The Marikina River Basin (outlined in black) located within the 120-km range of the S-band single-pol radar in Subic and the C-band dual-pol radar in Tagaytay..

Although there have been an increase on the use of weather radar data for hydrological applications over the past years, it is still not used as broadly as they should be (Berne and Krajewski, 2013). One major reason is the systematic and random errors in radar rainfall estimates that tend to translate into errors in hydrological models' simulated stream flow (Borga, 2002). In this study, we evaluated for the first time the potential of radar quantitative precipitation estimates (QPEs) from the

two different radar types – a dual-pol C-band and a single-pol S-band radars that both cover the MRB in forcing a continuous hydrological model. From C-band, two alternative radar products are generated: for the first, rainfall is estimated from attenuation and bias corrected reflectivity, $R(Z_C+PIA)$ (C subscript is to denote its C-band radar as source); for the second, rainfall is estimated from the specific differential propagation phase, $R(K_{DP-C})$. For the S-band radar, rainfall was estimated from bias corrected reflectivity $R(Z_S)$ (S subscript is to denote its S-band radar as source). As a benchmark, we estimated rainfall by interpolating rain gauge observations (Gauge only product, GO). Hydrological simulations are carried out for August 2012. This covers the huge flood event mentioned above. We used the Open Source software library *wradlib* (Heistermann et al. 2013b) for radar data processing. For hydrological modeling, we use the Eco-Hydrological Simulation Environment (ECHSE, Kneis 2014a), an Open Source tool designed for rapid development and deployment of hydrological simulation models. The overarching aim of this study is to identify which rainfall product is most suitable for simulating flood conditions in the Marikina River Basin.

2 Data and methods

2.1 Rainfall and discharge data

For the preparation of a calibrated hydrological model, we used hourly rain gauge and discharge data from 1994-2011 provided by the Effective Flood Control Operation and Services (EFCOS). The rain gauge data are from the five rain gauges within the MRB and the discharge data from the Montalban gauging station (refer to Fig. 1). For the comparative hydrological simulations, radar data from both radars are available for the contiguous period in August 2012. Technical specifications of the radar devices are listed in Table 1. Rain gauge data for the corresponding month are from the 19 newly-installed rain gauges from NOAA within and near MRB and the corresponding flow data are likewise from EFCOS.

Table 1: Technical specifications of the S-band single-pol radar and the C-band dual-pol radar.

	Subic S-band radar	Tagaytay C-band radar
Bandwidth	S-Band	C-Band
Polarization	Single –Pol	Dual-Pol
Position (lat / lon)	14.822°N 120.363°E	14.123°N 120.974°E
Altitude (m a.m.s.l.)	532	752
Maximum range	120 km	120 km
Azimuth resolution	1°	1°
Gate length	500 m	500 m
Number of elevation angles	14	14
Elevation angles	0.5°, 1.5°, 2.4°, 3.4°, 4.3°, 5.3°, 6.2°, 7.5°, 8.7°, 10°, 12°, 14°, 16.7°, 19.5°	0.5°, 1.5°, 2.4°, 3.4°, 4.3°, 5.3°, 6.2°, 7.5°, 8.7°, 10°, 12°, 14°, 16.7°, 19.5°
Volume cycle interval	8 minutes	15 minutes

2.2 Radar data processing

The estimation of rainfall from radar data was performed using the Open Source radar processing library *wradlib*. The library is composed of tools that allow rainfall retrieval for a multitude of applications (Heistermann et al. 2013b). Below is the brief description of the processing methods that were applied to derive the different rainfall products. For a more detailed description of the methods please refer to the library reference in <http://wradlib.bitbucket.org>.

2.2.1 Correcting for mean systematic bias

Both the S-band and the C-band were affected by serious hardware miscalibration. For the S-band radar, calibration bias was determined by comparison of the rainfall retrieved from the radar with rainfall observed by rain gauges, while for the C-band radar, a polarimetric self-calibration approach was applied that was based on Gorgucci et al. (1999). The S-band was found to be underestimated by 6 dB and the C-band by 8.5 dB.

2.2.2 Clutter Detection and removal

Removal of the non-meteorological echoes was done separately for each of the radars. For S-band radar, a static clutter map was based on the average reflectivity from a four-day period of clear-air conditions. For the C-band radar, the fuzzy echo classification procedure from Vulpiani et al. (2012) was used.

2.2.3 Differential phase processing

The approach used here is based on an iterative procedure presented by Vulpiani et al. (2012), which is now implemented in the *wradlib* function *dp.process_raw_phidp_vulpiani*. After removal of non-meteorological echoes, initial K_{DP} is

estimated from the raw Φ_{DP} profile by using a convolution filter. This initial K_{DP} profile is used to remove other artifacts and to unwrap the Φ_{DP} profile. After that step, K_{DP} estimation and Φ_{DP} reconstruction are repeated in three iterations.

2.2.4 Rain rate estimation

Here we give a brief description of the different methods in estimating rainfall from the different data sources. These produced different rainfall products which were later used for the hydrological simulations.

a. $R(Z_S)$ - Rainfall from reflectivity (from S-band)

After correcting for the systematic bias (section 2.2.1), reflectivity Z (dBZ) was converted to rainfall rate R (mm/h). We applied the $Z(R)$ relation suggested by the United States National Oceanic and Atmospheric Administration (NOAA) for tropical cyclones— $Z = 250 * R^{1.2}$

b. $R(Z_C + PIA)$ - Rainfall from attenuation corrected reflectivity (from C-band)

According to Bringi et al. (1990), the specific differential phase, K_{DP} , and the specific attenuation α_{hh} (dBkm⁻¹) are almost linearly related by coefficient γ_{hh} (dB deg⁻¹) by:

$$\alpha = \gamma_{hh} K_{DP} \quad (1.1)$$

Here we assumed γ_{hh} as constant in space and time with a value of $\gamma_{hh} = 0.08$, following the suggestion of Carey et al. (2000). The attenuation corrected reflectivity is later converted to rainfall intensity R using the procedure in the previous section (a).

c. $R(K_{DP-C})$ - Rainfall from specific differential phase (from C-band)

The estimation of rainfall from specific differential phase KDP was performed using the general expression suggested by Ryzhkov et al. (2005):

$$R = 129(|K_{DP}|/f)^{0.85} \text{sign}(K_{DP}) \quad (1.2)$$

d. GO - Rainfall from rain gauge observations

The gauge only (GO) product corresponds to the spatial interpolation of rain gauge observations using inverse distance weighting (see *adjust.GageOnly* and *ipol.Idw* in *wradlib*'s library reference).

2.2.5 Gridding and interpolation to sub-catchments

Rainfall estimates were retrieved from the three lowest elevation angles. From these, we created a Constant Altitude Plan Position Indicator (Pseudo-CAPPI) for an altitude of 2000 m a.s.l. by three-dimensional inverse distance weighting (based on the *wradlib* class *vpr.PseudoCAPPI*). In order to use the radar data as input to the hydrological model, we interpolated the gridded data again to the sub-catchment centroids by inverse distance weighting (IDW), with a power of 2.

2.3 The hydrological model

The Marikina River Basin hydrological model (MRB model) was developed using the model engine HYPSON-RR (Kneis, 2014a). This model engine is within the modelling framework software—Eco-Hydrological Simulation Environment (ECHSE) (Kneis, 2014b) and performs fast computations suitable for operational applications. The MRB model is a semi-distributed (discretization of 2.0 km² sub-catchment area and 1.8 km average reach length) conceptual model composed of a network of sub-catchments, reaches and nodes. The discretization is based on the SRTM elevation model (CGIAR, 2011) with 90 m resolution per pixel using a terrain pre-processor distributed with the ECHSE (Kneis 2014c). It follows the Xinanjiang approach (Zhao et al., 1980) in calculating for the run-off in a sub-catchment. The Leaf Area Index (LAI) which represents seasonal variation is used as a proxy for crop factors in calculating for the actual ET using Makkink model (de Bruin, 1987). A total of 15 catchment parameters are used for each sub-basin, seven of which were independently calculated and the rest were calibrated using hourly precipitation and discharge data from 1994-2011. We used a sequence of Monte-Carlo simulations based on the strategy of Kneis et al. (2014).

However, model calibration can offset errors from input variables (e.g. rainfall) such that parameters “adapt” to the specific forcing used during the calibration (Heistermann and Kneis, 2011). Thus, for a fair comparison of the performance of the model using the different rainfall inputs, we re-calibrated the model for each of the rainfall products. We used the different rainfall products to force our model, with emphasis on the *Habagat* event that occurred during the month of August. To measure the quality of the simulated flows compared to the observed flows, we employed the percentage bias (pBias) and Nash-Sutcliffe Efficiency (NSE) with the following equations:

$$pBias = \frac{\frac{1}{n} \sum_{i=1}^n (q_i - o_i)}{\omega} \cdot 100\% \quad (1.3)$$

$$NSE = 1 - \frac{\sum_{i=1}^n (q_i - o_i)^2}{\sum_{i=1}^n (o_i - \omega)^2} \quad (1.4)$$

Where q_i is the i th out of n simulated discharge, o_i is the observation corresponding to q_i , and ω the mean of all n observations.

3 Results and discussions

The three radar rainfall products showed similar spatial pattern albeit different values in contrast to the spatial pattern derived from the rain gauge observations (Fig.2). The S-band radar shows a systematically high precipitation estimates compared to the other rainfall products. This could be attributed to the miscalibration of the radar hardware.

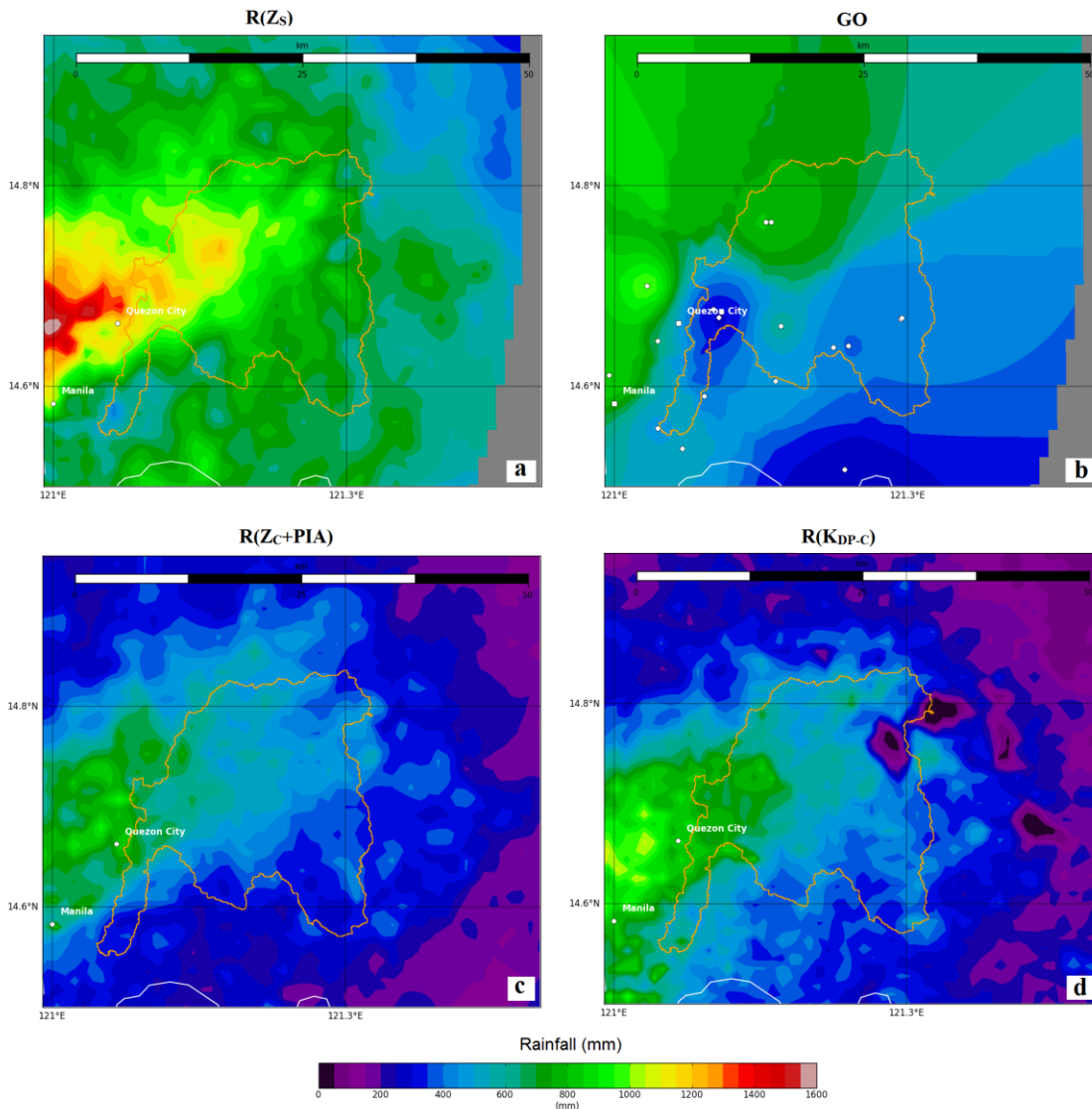


Figure 2: Maps for accumulated rainfall for the Habagat event (Aug 06-09) from different rainfall products: (a) $R(Z_s)$, (b) GO , (c) $R(Z_c+PIA)$, and (d) $R(K_{dp,c})$ in the MRB. White circles in (b) are the locations of rain gauges used to generate the GO product.

The accumulated mean areal rainfall during the *Habagat* shows that MRB received at least 600 mm of rainfall in a span of four days (Fig.3). The different rainfall products showed the same trend of rainfall accumulation through time, although the C-band dual-pol radar products have lower estimates compared to both the $R(Z_s)$ (based on S-band reflectivity) and GO products.

In terms of hydrological simulations, all the simulated stream flows from the different rainfall products show a good agreement with the observed stream flows for the given time period (Fig. 4). The $R(Z_s)$ product (based on S-band

reflectivity) well-captures the shape and magnitude not only of the major flood hydrograph during the flood of *Habagat* event but also the low flows during the entire month.

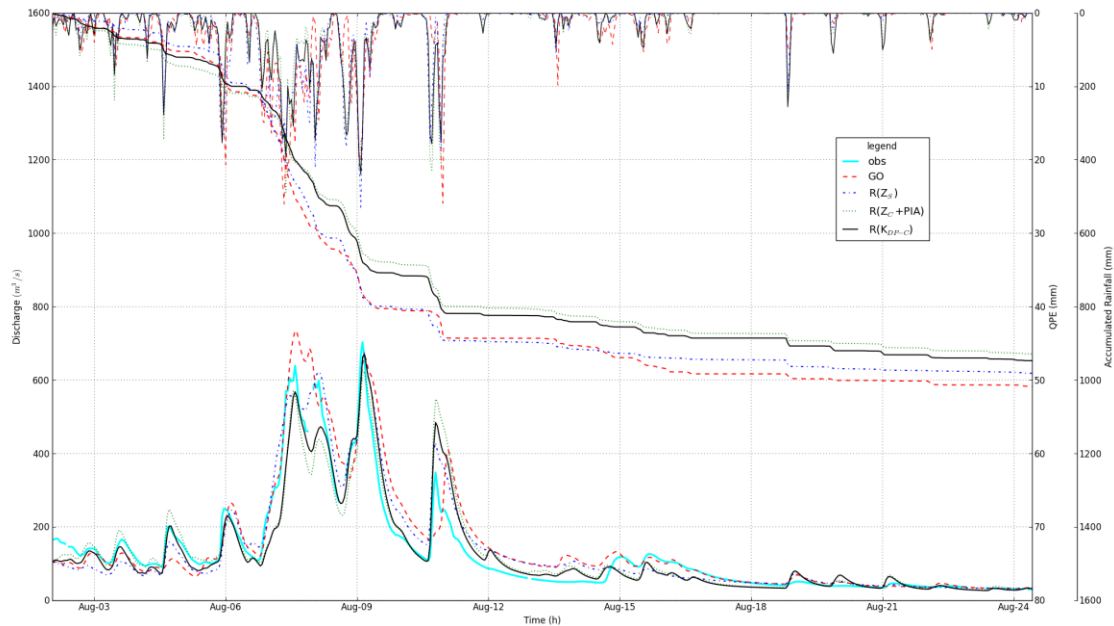


Figure 3: Simulated flows from different rainfall products and the observed flows during the month of August, 2012. Accumulated mean areal rainfall and hourly QPEs from the different rainfall products are also plotted.

In particular, for the entire month of August, the $R(Z_S)$ product performs best among the four inputs in terms of NSE value of 0.88 while the GO product performs comparatively weak with 0.79 NSE and an overestimation of 13.4 % (Tab. 2). The pBias value for the $R(Z_C+PIA)$ is notably 0.0 % and $R(Z_S)$ and $R(K_{DP-C})$ perform well with only slight overestimation of 6.4% and an underestimation of 2.8% respectively. For the *Habagat* event we made the comparison of flows for the time frame Aug 06-12 to account for the recession stage of the event. Based from calculated goodness of fit values the trend of performance is similar to the results for the entire month of August. There is however a slight decrease in the values of NSE and pBias for all the rainfall products, most strikingly for simulated flows from $R(Z_C+PIA)$ which NSE value decreased from 0.82 for the entire month of August to 0.71 for the *Habagat* event (Tab 2).

Table 2: Performance of the different QPEs in driving the MRB hydrological model for the *Habagat* event (Aug 06-12) and for the entire month of August 2012.

QPE product	NSE		pBias (%)	
	<i>Habagat</i>	August 1-25	<i>Habagat</i>	August 1-25
GO	0.68	0.79	21	13.4
$R(Z_S)$	0.86	0.88	16.2	6.4
$R(Z_C+PIA)$	0.71	0.82	-0.7	0.0
$R(K_{DP-C})$	0.81	0.86	1.4	-2.8

4 Conclusions and outlook

In this study we retrieved different rainfall products from different sources—rain gauge observations, S-band radar, and C-band dual-pol radar in order to test their performance in simulating stream flows. We performed the rainfall estimations using the tools in the open source radar processing software *wradlib*. We focused our analysis on the Marikina River Basin which is within the range of both radars and is well monitored by rain gauge and river discharge gauges. The wettest month of the year (August) in 2012, where a huge monsoon-induced rainfall event occurred is considered as the simulation time frame.

A calibrated continuous hydrological model was prepared for the analysis to test the applicability of the HYPISO-RR model engine in the Philippines. The model was recalibrated for each of the rainfall product to remove the bias in the parameter estimations, allowing for a fair comparison of the performance of the different rainfall products.

The retrieved rainfall estimates showed that the S-band radar is systematically producing higher precipitation values than the rest of the rainfall products. We assume that this could be an effect of hardware miscalibration. Based on the simulated flows, the rainfall product from the S-band single-pol radar $R(Z_S)$ outperforms the rest in terms of NSE value and a minimal

overestimation of 6.4%. The rainfall from the attenuation corrected reflectivity from C-band dual-pol R(Z_C+PIA) on the other hand produced a 0.0% bias. The rainfall retrieved from differential phase processing R($K_{DP,C}$) also performed fairly well with 0.86 NSE. The rainfall input from the rain gauge observations GO was the weakest producing a 0.79 NSE and the biggest bias of 13.4%. Similar quality of performance is apparent with the *Habagat* event, which implies that even for flood flows, the radar rainfall products outperform the GO product.

The performance of the radar rainfall products has shown that, with adequate processing, both radar sources are suited for hydrological simulations at least in the Marikina River Basin. Now the challenge is to verify this applicability for other radar stations and catchments in the Philippines.

Acknowledgement

We would like to thank the Philippine Atmospheric, Geophysical and Astronomical Services Administration (PAGASA) for generously providing the radar data. The NOAA (National Operational Assessment of Hazards) project and the EFCOS (Effective Flood Control Operation and Services) provided the rain and river gauge data. This study is funded by Helmholtz Association through the GeoSim graduate research school. We also thank Bernard Allan Racoma, Justine Perry Domingo, Pamela Tolentino, Mark Clutario, Joan de Vera, Gerald Quiña, and Carlo Manalansan for assisting in the field works.

References

- Berne A., and Krajewski W.F.** Radar for hydrology: Unfulfilled promise or unrecognized potential? *Adv in Water Res.* 2013. Vol. 51. 357-366
- Bringi, V. N., V. Chandrasekar, N. Balakrishnan, and D. S. Zrnice.** An examination of propagation effects in rainfall on radar measurements at microwave frequencies. *J. Atmos. Oceanic Technol.* 1990. Vol. 7. 829-840.
- Carey, L. D., S. A. Rutledge, and D. A. Ahijevych.** Correcting propagation effects in C band polarimetric radar observations of tropical convection using differential propagation phase. *J. Appl. Meteor.* 2000. Vol. 39. 1405-1433.
- CGIAR-CSI-Consortium of International Agricultural Research Center- Consortium for Spatial Information, SRTM Data downloads.** 2011. <http://srtm.csi.cgiar.org/SELECTION/listImages.asp>. URL visited 07.12.2011
- de Bruin, H.A.R.** From Penman to Makkink, In: *Evaporation and Weather: Proceedings and Information.* 1987. No. 39, edited by: Hooghart, J. C., TNO Committee on Hydrological Research, The Hague, 1191.
- Gorgucci, E., G. Scarchilli, and V. Chandrasekar.** A procedure to calibrate multiparameter weather radar using properties of the rain medium, *IEEE Transactions On Geoscience And Remote Sensing.* 1999. Vol. 37(1). 269-276.
- Heistermann M., Crisologo I., Abon C.C., Racoma B.A., Jacobi S., Servando N.T., David C.P.C., and Bronstert, A.** Brief Communication: Using the new Philippine radar network to reconstruct the “Habagat of August 2012” monsoon event around Metropolitan Manila. *Nat Hazards Earth Syst Sci.* 2013b. Vol. 13. 653-657 doi:10.5194/nhess-13-653-2013
- Heistermann, M., Jacobi, S., and Pfaff, T.** Technical Note: An open source library for processing weather radar data (wradlib), *Hydrol. Earth Syst. Sci.* 2013b. Vol. 17. 863-871.
- Heistermann M, Kneis D,** Benchmarking quantitative precipitation estimation by conceptual rainfall-runoff modeling. *Water Resour Res.* 2011. 47 :W06514 doi:10.1029/2010WR009153
- Borga M.** Accuracy of radar rainfall estimates for streamflow simulation. *J Hydrol.* 2002. Vol. 267. 26-39
- Kneis, D.** Eco-Hydrological simulation environment (ECHSE), Documentation of model engines. Institute of Earth and Environmental Sciences, University of Potsdam, Germany. March 2014a. http://echse.bitbucket.org/downloads/documentation/echse_engines_doc.pdf - URL visited 10.06.2014
- Kneis, D.** Eco-Hydrological simulation environment (ECHSE), Documentation of the Generic Components, Institute of Earth and Environmental Sciences, University of Potsdam, Germany. May 2014b. http://echse.bitbucket.org/downloads/documentation/echse_core_doc.pdf - URL visited 10.06.2014
- Kneis, D.** Eco-Hydrological simulation environment (ECHSE), Documentation of Pre- and Post-Processors, Institute of Earth and Environmental Sciences, University of Potsdam, Germany. March 2014c. http://echse.bitbucket.org/downloads/documentation/echse_toos_doc.pdf - URL visited 10.06.2014
- Kneis, D., Chatterjee, C., and Singh, R.** Evaluation of TRMM rainfall estimates over a large 485 Indian river basin (Mahanadi), *Hydrol. Earth Syst. Sci. Discuss.* 2014. Vol. 11. 1169-1201, doi:10.5194/hessd-11-1169-2014.
- Liongson L.Q.** Flood mitigation in Metro Manila. *Philippine Engineering Journal.* 2008. Vol. 29(1). pp. 51-66
- NDRRMC – National Disaster Risk Reduction and Management Council** SiteRep No. 20 re Effects of Southwest Monsoon (HABAGAT) Enhanced by Tropical Storm “Maring”. 2013.
- PAGASA – Philippine Atmospheric Geophysical and Seismological Administration.** 2004 <http://kidlat.pagasa.dost.gov.ph/cab/climate.htm>. URL visited 19.06.2013
- Ryzhkov, A. V., S. Giangrande, and T. J. Schuur.** Rainfall estimation with a polarimetric prototype of WSR-88D. *J. Appl. Meteor.* 2005. Vol. 44. 502-515.
- Vulpiani, G., M. Montopoli, L. D. Passeri, A. G. Gioia, P. Giordano, F. S. Marzano.** On the Use of Dual-Polarized C-Band Radar for Operational Rainfall Retrieval in Mountainous Areas. *J. Appl. Meteor. Climatol.* 2012. Vol. 51. 405-425.
- Zhao, R.-J., Zuang, Y.-L., Fang, L.-R., Liu, X.-R., and Zhang, Q.-S.** The Xinanjiang model, 30 in: *Hydrological Forecasting, Proceedings of the Oxford Symposium, of IAHS-AISH Publ., IAHS Press, Wallingford, UK.* 1980. Vol. 129. No. 1191. 351-356.